Astron. Astrophys. 293, 572–576 (1995)

ASTRONOMY AND ASTROPHYSICS

Frequency–time analysis of solar irradiance and activity indices

A.V. Mordvinov

Institute of Solar-Terrestrial Physics, P.O.Box 4026, Irkutsk 33, 664033, Russia

Received 9 December 1993 / Accepted 21 May 1994

Abstract. The power spectrum of total solar irradiance is studied and compared to spectra of other solar global parameters. These have false periodicities originating from the rotation and hence convolution of the spatial distribution of the features on the solar disk and the limb-darkening function. Ranges for which the spectral density follows a power-law are identified and the fractal dimension is estimated. The time-varying nature of the periodicities is illustrated by comparing the dynamic spectra of the irradiance and activity indices. They show consistent features presented in global parameters. Both coherence and transfer function modulus of the solar mean magnetic field (SMMF) and the total irradiance are estimated. From the results of this analysis, it is concluded that these parameters are causally related.

Key words: activity of the Sun – magnetic fields – method: data analysis

1. Introduction

High-precision and long-term "solar constant" measurements have shown that total solar irradiance varies over a wide range of time scales: from minutes to more than a decade (Fröhlich 1992; Makarova et al. 1991). The main contribution to irradiance variability is related to sunspot radiation deficit and the irradiance excess due to faculae (e.g. Willson et al. 1981). These main factors are not independent: they are combined into active regions and are linked during their evolution.

The total irradiance time variations are controlled by other factors as well, such as velocity and magnetic fields beneath the photosphere, which regulate the convective heat transport, and possibly energy generation changes in the solar core. Fröhlich & Pap (1989) revealed significant relations between the total irradiance, the 10.7 cm radio flux ($F_{10.7}$), equivalent width of the He-line at 1083 nm, and the ultraviolet irradiance. These relations characterize the influence of many effects on solar irradiance. Under the influence of all these factors a broad power spectrum results which is related to the dynamic process time scales in, above, and below the photosphere.

The solar activity indices are usually analysed in the time or frequency domains. Classical spectral analysis is not the best method for studying solar time series because of its non-steady behaviour. Bouwer (1992) applied time windowed frequency analysis to study many solar parameters. His results indicate that both amplitudes and periods of solar oscillations vary over the solar cycle. This method is appropriate for quasi-stationary processes, and the time resolution is determined by the window's length and not by the shift of its position. In this paper we use a dynamic analysis besides the ordinary spectral analysis. This method provides the spectral characteristics as functions of the frequency and time (Dziewonski et al. 1969) and the resolution is only limited by the uncertainty principle.

A comparative study of dynamic spectra is presented for solar irradiance from the Nimbus-7, $F_{10.7}$, relative sunspot numbers R, and solar mean magnetic field (SMMF). Solar irradiance data are from Hoyt et al. (1992) evaluated according to their new algorithm. The time series of $F_{10.7}$, R, SMMF are from the Solar Geophysical Data and cover the period from November 16, 1978 to June 17, 1992.

2. Spectra of irradiance and SMMF

The total solar irradiance power spectrum is presented in Fig. 1a in log–log plane. The power spectrum is normalized in such a way that the maximum value corresponds to 0 decibel. There are small peaks in the spectrum which overlie the continuous background which is decreasing with the frequency. The spectrum can be devided into three regions, which are produced by different physical factors. At low frequencies the main peak corresponds to a period of 11.2 years, obviously caused by the total irradiance variations with the solar cycle. In the middle part of the spectrum with periods ranging from about one month to two years spectral density consists of small peaks overlaid on a power-law background

$$g(f) = \text{const} \cdot f^{-\gamma}, \quad (1)$$

with $\gamma \approx 0.25$ (indicated by the dashed line). There are peaks corresponding to the solar rotation period $P = 27 - 31$ d and the period doubled. This spectral range is characterized by time scales of the evolution of active regions and complexes.

Convection drives most of the large-scale motions beneath the photosphere, and convective motions control and influence

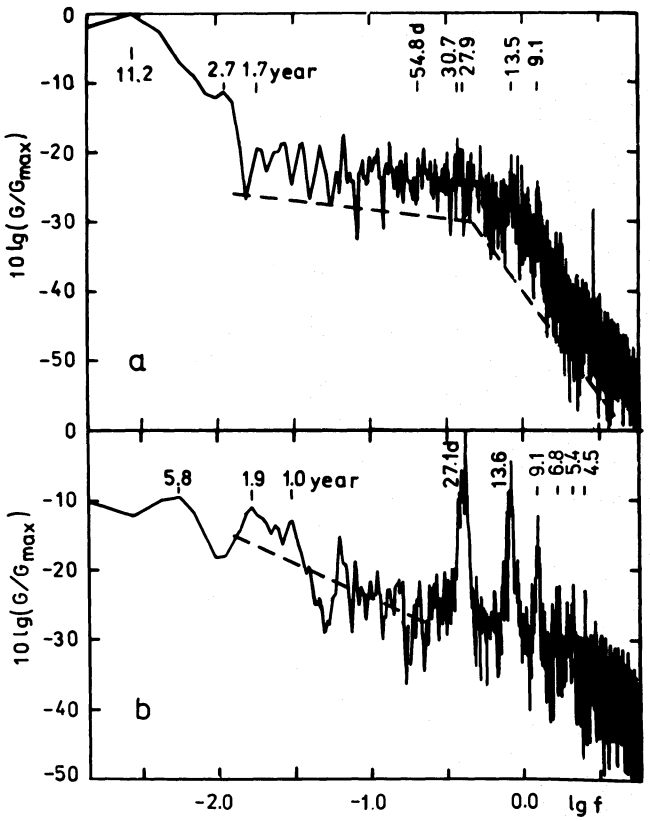

Fig. 1a and b. Power spectrum of solar irradiance (**a**); and of solar mean magnetic field (**b**). The dominant periods are indicated on the top of each plot. The dashed lines indicate the power-law for the evaluation of γ according to Eq. (1)

the activity phenomena, which are ordered in space and in time in accordance with the convective scales. Thus the magnetic field distribution displays the large-scale velocity fields beneath the photosphere (McIntosh & Wilson 1985), and some peaks in the solar irradiance spectrum are caused by such coherent global convection structures which can even exist in a fully turbulent hydrodynamic flow and modulate the heat transport. Therefore the characteristic scales of convection should manifest themselves in the total irradiance variability. The peaks at 1.73 and 2.79 year periods could be related to quasi-biennial periodicities which are presented in variations of many solar and geophysical parameters (Apostolov 1985). Mordvinov (1987) proposed an interpretation of these quasi-biennial oscillations as the result of activity parameter modulation by large-scale convective cells. Some peaks in this region could also be the result of $r-$ and $g-$modes as indicated by Wolff & Hickey (1987).

At higher frequencies, when periods are less than the solar rotation period, the power spectrum slope becomes steeper with $\gamma \approx 4.1$. At these frequencies, the spectrum is due to inherent time variations and to brightness inhomogeneities on the visible disk modulated by solar rotation. The time derivative of the irradiance F is given by $\mathrm{d}F/\mathrm{d}t = \partial F/\partial t + (\boldsymbol{v}\nabla)F$, where the first term represents the temporal variation itself and the second one the rotational modulation that is the transport of F from the invisible solar hemisphere to the visible one and vice versa. The spatial periodicity of brightness distribution in heliographic longitude leads to irradiance variations at a frequency $f \approx k/P_\mathrm{c}$ related to the Carrington rotation period P_c, and the wave number k of the inhomogeneity. The peak at $P = 13.5$ d, e.g., is caused by the quadrupole component of the activity distribution (Donnelly & Puga 1990). Thus, the rotation of the Sun transforms the spatial spectrum of brightness inhomogeneities into the frequency spectrum of total irradiance. There is a set of peaks P_i in activity indices spectra corresponding to overtones of the rotation period: $P_i \approx P_\mathrm{c}/i$, $i = 1, 2, \ldots$ (Fröhlich & Pap 1992; Rivin & Obridko 1992). At least three of these peaks are observed in the solar irradiance spectrum (Fig. 1a) and in spectra of other solar parameters (Fröhlich & Pap 1989).

Figure 1b shows the power spectrum of the SMMF time series which were obtained at Stanford observatory for the same time interval. The gaps in data were filled by the use of time series modelling according to the algorithm by Fahlman & Ulrych (1982). The power law of the middle range corresponds to $\gamma \approx 1$. There are also peaks at quasi-biennial and annual periods on top of the power-law background. The peak at $P \approx 27.1$ d dominates the spectrum, which has a complicated structure related to different rotational modes (Kotov & Levitsky 1983). At higher frequencies a set of overtone peaks at P_i is seen until $i = 6$.

3. The origin of false periodicities

Let the distribution of any parameter over the solar disk be described by the function $F(\lambda, \varphi, t)$ where λ, and φ are the heliographic longitude and latitude. The observed signal $\overline{F}_t$ results from the convolution of $F(\lambda, \varphi, t)$ with a weighting function W, which includes the limb darkening function $\beta(\theta)$, with θ the angular distance from the solar disk center

$$\overline{F}_t = \int_{-\pi/2}^{\pi/2} F(\lambda, \varphi, t)\, W(\theta)\, \mathrm{d}\theta\,. \tag{2}$$

With the limb darkening function of Allen (1973), $W(\theta)$ becomes for the visible part:

$$W(\theta) = 0.46 + 0.86\cos\theta - 0.20\cos^2\theta\,, \quad |\theta| \le \pi/2\,, \tag{3}$$

and $W(\theta) = 0$ for the invisible part ($\pi/2 < |\theta| \le \pi$). Based on Eqs. (2) and (3) a numerical experiment was carried out, in which only longitudinal and temporal variations were taken into account. The equatorial part of the Sun, that mostly influences the total signal, was represented by a cylinder rotating with P_c. The observed parameter was assumed to change stochastically, i.e. F is a random function. For daily observations F_i is defined at equally spaced longitude intervals $\Delta\lambda = 2\pi/P_\mathrm{c}$. The observed signal becomes approximately

$$\overline{F}_i = \sum_{k=-L}^{L} F_{i+k} W_k\,, \tag{4}$$

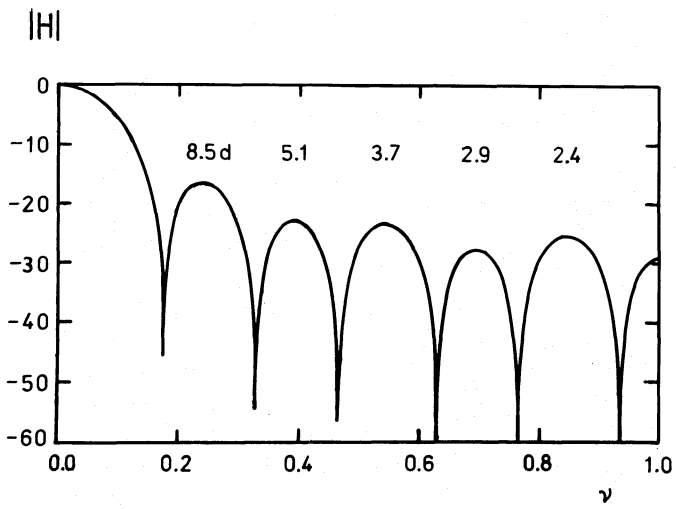

Fig. 2. Normalized filter's gain versus dimensionless frequency $\nu = f/f_N$, where f_N is the Nyquist frequency corresponding to a 1 day sampling

with $L = 6$ the number of values east/west of the central meridian. F_i is the input time series and $\overline{F}_i$ is the output after filtering by Eq. (4). Thus, the integration of the parameter over the solar disk is equivalent to the application of a linear filter on the time series. The filter's gain $|H(f)|$ may be determined from the input and output spectral densities $S_x(f)$, $S_y(f)$ (Otnes & Enochson 1978)

$$|H(f)| = \sqrt{S_y(f)/S_x(f)}\,. \tag{5}$$

Randomly distributed F_i ($i = 1, 2, \ldots, 4096$) were used as input time series. Figure 2 shows the results of this simulation in terms of the filter's gain versus frequency. There are five peaks besides the main one at periods of 8.5, 5.1, 3.7, 2.9, 2.4 days. In spite of the rough simplification the derived periodicities are close to the observed ones. This numerical experiment demonstrates that even a randomly varying parameter leads to "false" periodicities due to the rotation and convolution with the limb darkening function.

4. Dynamic spectra

Frequency-time analysis (Dziewonski et al. 1969) is an effective method to analyze non-steady time series. Dynamic spectra have been used to characterize, e.g., the spectral and time properties of solar activity (Mordvinov 1988).

The dynamic spectrum is given by

$$Y(\omega_k, t) = \frac{1}{\pi}\int_0^\infty B\left[(\omega-\omega_k)/\omega_k\right] S(\omega)\exp(i\omega t)\mathrm{d}\omega\,, \tag{6}$$

where $S(\omega)$ is the Fourier transform of the time series being analysed, $B\left[(\omega-\omega_k)/\omega_k\right] = \exp\{-\alpha[(\omega-\omega_k)/\omega_k]^2\}$ the frequency characteristic of the bandpass filter centered on frequency ω_k and α characterizing the bandwidth of the filter.

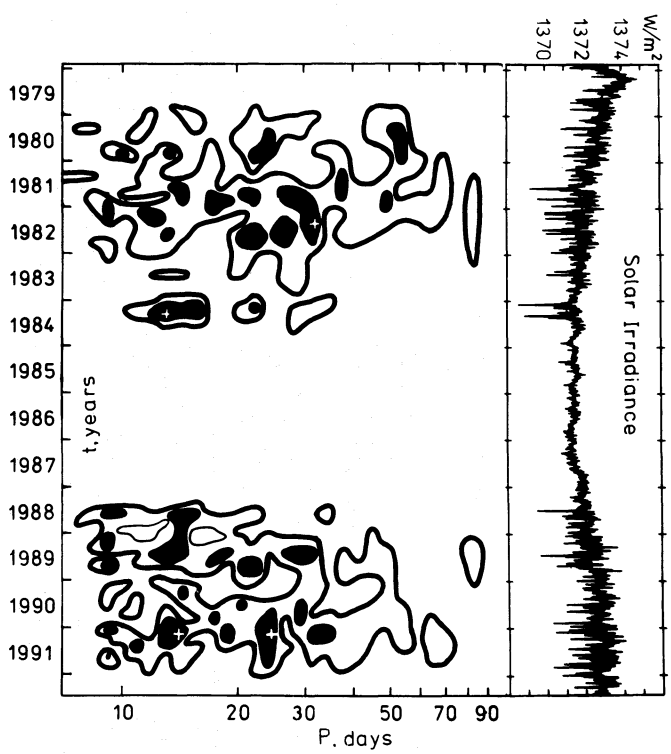

Fig. 3. Dynamic spectrum of solar irradiance. The isolines are plotted for 5 and 10 decibel. The main maxima are marked by crosses

The dynamic spectrum of total solar irradiance $|Y(P,t)|$ in terms of period P is shown in Fig. 3. Values of $|Y(P,t)|$ are again normalized to the maximum value. According to the uncertainty principle, spectral characteristics make sense if averaged over an area of $2\delta_t \times 2\delta_P$ in (P,t)-plane. Uncertainties in time and period are $\delta_t \approx 63$ d and $\delta_P \approx 1$ d for $\alpha = 200$ at $P = 20$ d. The uncertainty δ_P is larger than the resolution of spectral analysis over the full period of time, but this analysis offers the possibility of studying the dynamics of non-steady time series. There are two regions with enhanced power corresponding to the maxima of the activity cycles 21 and 22. The energy distribution changes during the 11-year cycle and from cycle to cycle as well, and is concentrated within the range of periods from 8 days to 3 months. The main maxima of the dynamic spectra (0 dB) are found at about $P = 13.5$ d in both cycles (1984 and 1991). The next maxima (≈ 1 dB) are at $P \approx 31$ d in 1982 and at $P \approx 24$ d in 1991. In cycle 22 the dynamic spectrum maxima are delayed by about one year from the sunspot number maximum epoch; for cycle 21 the maxima are delayed by even more, about two and four years.

In Fig. 4 the dynamic spectra of sunspot numbers R, $F_{10.7}$, and SMMF are overlaid on the irradiance spectrum. Isolines are plotted for the 8 dB level which corresponds to e times less than the maximum value. It is interesting to note that the 27-day variation predominating in all activity indices is only barely manifested in solar irradiance.

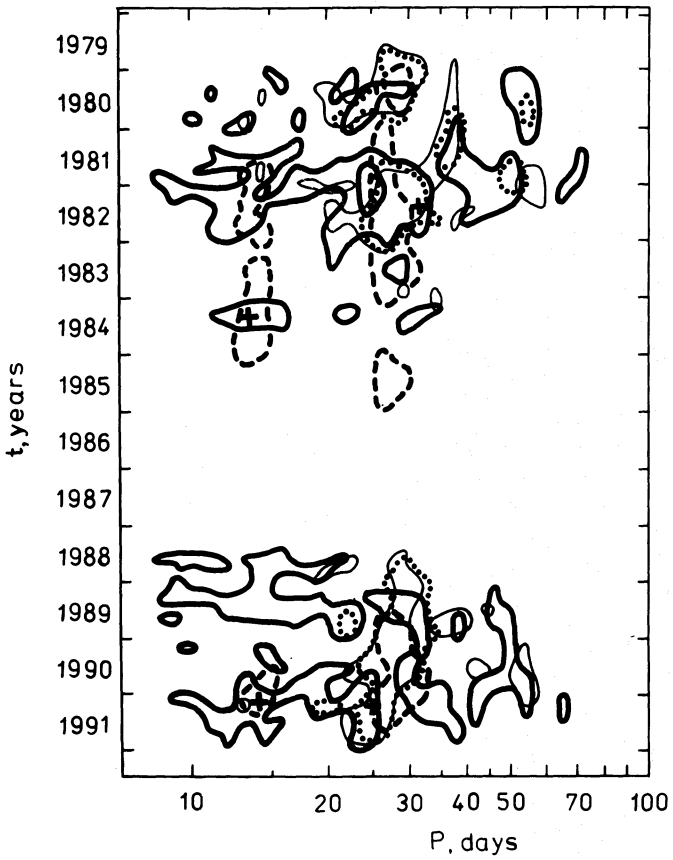

Fig. 4. Dynamic spectra of solar irradiance, relative sunspot numbers R, $F_{10.7}$ and SMMF plotted as heavy, light, dotted, and dashed lines, respectively

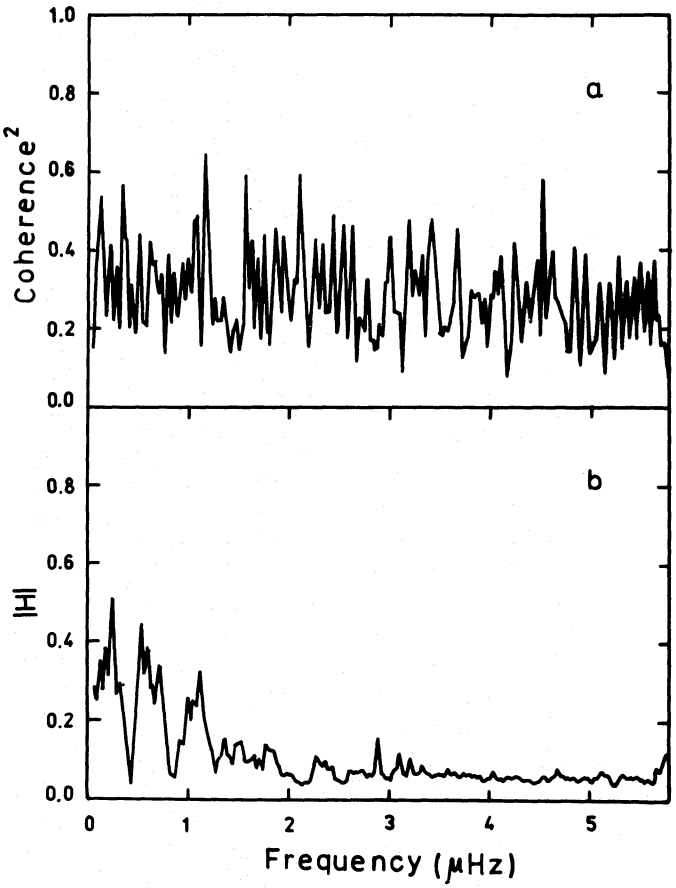

Fig. 5a and b. Coherence squared (**a**) and the transfer function modulus (**b**) of the association between solar irradiance and SMMF

During the solar cycle activity zones drift towards the equator according to Spörer's law; thus the synodic rotation period changes from about 30 to 27 d during 2–3 years and structures with a corresponding tilt are clearly seen in dynamic spectra of sunspots R and $F_{10.7}$. Some features in dynamic spectra of solar irradiance and SMMF overlap at $P \approx 13.5$ d in 1981–1982, 1984, and 1990–1991. In particular, the main maxima for solar irradiance in 1984 and 1991 are located close to local ones of the SMMF. In the first half of 1984, there were two activity complexes on the Sun located directly opposite in longitude, and accordingly there was a four-sector background magnetic field structure. From the end of 1990 to mid-1991, the distribution of active regions was complicated, and so was the dynamic spectrum structure.

Figure 4 clearly illustrates that the dynamic spectra of all indices sometimes exceed −8 dB at periods from 25 to 31 d, the period of solar rotation. In 1982 the maximum of the solar irradiance dynamic spectrum was located close to this period; in 1991 only the second maximum of $|Y(P,t)|$ occured there. However, the joint effect of different factors at the rotational period leads to an increase in solar irradiance variation.

5. The SMMF and solar irradiance as linear system input and output

The consistent features in the frequency-time space give evidence for a causal relation of the SMMF and solar irradiance, which has its physical basis: large-scale magnetic fields influence the convection and reduce the heat transport. Weak magnetic fields, however, suppress turbulent viscosity and increase the heat transport and the balance of both effects determines the net effect on irradiance. Besides, there are also direct physical relations of magnetic and thermodynamic phenomena (Landau & Lifshitz 1982). At present it is difficult to evaluate from a theoretical point of view the contributions of the different effects. A direct approach is to determine this relation by its linear association. The spectral coherence squared between SMMF and solar irradiance was estimated to describe this association. Fröhlich & Pap (1989) applied an analogous analysis to evaluate the associations with other activity indices. Figure 5 shows the coherence squared and the modulus of the transfer function. The latter was determined using Eq. (5) with the SMMF regarded as the input of some physical linear system and solar irradiance as output. For an equivalent degree of freedom $n = 50$ the 90 per cent confidence limits for coherence squared of 0.5 are 0.27 and 0.67. The gain error at $|H| = 0.5$ is about 0.16. The errors seem to

be rather large and both the coherence and gain are statistically not very significant over the whole time interval. The fact that there are obviously consistent features in the frequency-time space and the insignificant coherence could imply that a temporary varying or nonlinear relation exists between the parameters. The gain increases with decreasing frequency, which could indicate that long-term variations of both parameters are closely connected and may originate from the same physical cause.

6. Conclusions

The existence of power-law dependence of the total solar irradiance spectral density indicates a statistical self-similarity and fractal properties of the time series (Feder 1988). With the determined spectral index γ from Eq. (1) one can estimate the fractal dimension of the solar irradiance variability using the relation $\gamma = 2(1 - D)$ (McHardy & Czerny 1987). For the middle part of the spectrum the fractal dimension is $D = 0.875$. This value is larger than it is for flicker-noise $D_f = 0.5$, and less than that of the white-noise $D_w = 1.0$. Based on the self-similarity and scale invariance within the frequency ranges, one can conclude that time variations have some universal properties over a wide range of time scales. Perhaps, this self-similarity is related to fractal properties of large-scale convection, which covers a wide range of spatial and temporal scales and determines the energy transport.

At periods shorter than the solar rotation period, the time variability by itself adds up to the variance due to the rotational modulation of spatial inhomogeneities. As a result, the slope of the spectral density changes. The integration of the solar irradiance or the SMMF over the solar disk corresponds to a convolution of the observed parameter with the limb darkening function and leads to "false" periodicities in power spectra at periods of about 9 d and shorter.

The dynamic spectrum structure is mainly determined by the longitudinal distribution of activity and the rotation of the Sun, and by the temporal evolution of the activity. Main spectral maxima are found at a period of about 13.5 d and are caused by longitudinal activity inhomogeneities. A comparative analysis reveals consistent frequency and temporal behaviour of both solar irradiance and SMMF which leads to the conclusion of a causal relation between these parameters.

Acknowledgements. I thank Drs. G.V. Kuklin and L.A. Plyusnina for useful comments. I am especially grateful to the referee, Dr. C. Fröhlich, for his very useful remarks. Also, I would like to thank J. Sutton and K. Shaffer for improving the manuscript, and the U.S. scientists for making it possible to process their data. This research was supported in part by the Russian Fundamental Science Foundation under grant no. 93023114.

References

Allen C.W., 1973, Astrophysical quantities. Athlone, London
Apostolov E.M., 1985, Bull. Asron. Inst. Czech. 36, 199
Bouwer S.D., 1992, Sol. Phys. 142, 365
Donnelly R.F., Puga L.C., 1990, Sol. Phys. 130, 369
Dziewonski A., Bloch S., Landisman M., 1969, Bull. Seismol. Soc. Amer. 59, 427
Fahlman G.G., Ulrych T.J., 1982, MNRAS 199, 53
Feder J., 1988, Fractals, Plenum Press, New York
Fröhlich C., 1992, Solar Irradiance Variability, in: Donnelly R.F. (ed.) Proc. Workshop on the Solar Electromagnetic Radiation Study for Solar Cycle 22. NOAA ERL, Boulder, p. 1
Fröhlich C., Pap J., 1989, A&A 220, 272
Hoyt D.V., Kyle H.L., Hickey J.R., Maschhoff R.H., 1992, J. Geophys. Res., 97, 51
Kotov V.A., Levitski L.C., 1983, Long-term coherent periodicities in the mean magnetic field of the Sun, in: Stenflo J.O. (ed.) Proc. IAU Symp. 102, 23. Solar and Stellar Magnetic Fields: Origin and Coronal Effects, Reidel, Dordrecht, p. 23
Landau L.D., Lifshitz E.M., 1975, Electrodynamics of Continuous Media, Pergamon Press, Oxford, New York
Makarova E.A., Charitonov A.V., Kazachevskay T.B., 1991, Potok solnechnogo izlucheniya, Nauka, Moscow
McHardy I., Czerny B., 1987, Nat 325, 696
McIntosh P.S., Wilson H.R., 1985, Sol. Phys. 97, 59
Mordvinov A.V., 1987, Solnechnye dannye 11, 83
Mordvinov A.V., 1988, Issledovaniya po geomagnetizmu, aeronomii i fizike Solntsa 83, 134
Otnes R.K., Enochson L., 1978, Applied time series analysis, Wiley, New York
Rivin U.R., Obridko V.N., 1992, AZh 69, 1083
Willson R.C., Gukis S., Janssen M., Hudson H.S., Chapman G.A., 1981, Science 211, 700
Wolff C., Hickey J.R., 1987, Sol. Phys. 109, 1